Available online at www.sciencedirect.com
ScienceDirect
Planetary and Space Science 55 (2007) 1299–1309
Planetary and Space Science
www.elsevier.com/locate/pss

Hydrostatic, isothermal planetary models from the point of view of dynamical systems: "Determination of explicit formulas for the point of critical mass"

Johannes Schönke*

Arbeitsgruppe für nichtlineare Dynamik, Institut für Theoretische Physik der Universität Bremen, Germany

Received 11 September 2006; received in revised form 2 April 2007; accepted 13 April 2007
Available online 19 April 2007

Abstract

We investigate a planetary model in spherical symmetry, which consists of a solid core and an envelope of ideal and isothermal gas, embedded in a gaseous nebula. The model equations describe equilibrium states of the envelope. So far, no analytical expressions for their solutions exist, but of course, numerical results have been computed. The point of critical mass, above which no more static solutions for the envelope exist, could not be determined analytically until now. We derive explicit formulas for the core mass and the gas density at the core surface, for the point of critical mass. The critical core mass is also an indicator for the ability of a core to keep its envelope when the surrounding nebula is removed, because at this point, the core's influence extends up to the outer boundary at the Hill radius.

Keywords: Planet formation; Solar system; Autonomous dynamical systems; Point transformations

0. Introduction

In recent years, planet formation has raised a lot of new questions due to observational advances like the discovery of extra-solar gas giants. In the nucleated instability hypothesis, gas envelopes are formed around planetary cores, which in turn are built up by accretion of km-sized solid bodies. The envelope structure has been investigated with hydrostatic models, e.g. by Ikoma et al. (2001), Mizuno (1980), Papaloizou and Terquem (1999), Stevenson (1982), Wuchterl (1993). There was found an upper mass limit for static envelopes—the critical mass—above which no static solutions exist for given nebula conditions. The dependence of this critical mass on nebula conditions or material properties (opacities) is a quite complex problem. In the isothermal idealization used in this article, we can make an analytical approach, giving us deeper insights into the basic features of core–envelope structures and especially the critical mass.

As there are several definitions of the critical mass and the respective critical core mass (CCM) (cf. Wuchterl, 1991), we have to specify what we mean with "critical mass". We follow the definition introduced by Mizuno (1980) where the CCM is defined as the first maximum of $M_c(M_{tot})$. For a given total mass M_{tot} an eigenvalue problem is solved, giving the respective core mass M_c. Out of a series of increasing total masses a relation $M_c(M_{tot})$ arises. If this relation has a maximum, a contradiction occurs. Seen as a quasi-static time evolution, the core mass is a constantly growing structure but the maximum shows that there is no static solution for a core mass above the maximum, so this core mass is called the critical one after Mizuno (1980), hereafter called "classical" CCM. This definition makes no statements about the further evolution of a critical configuration, only the static possibilities are ruled out. It should be noted that the described procedure to get the CCM is done for fixed nebula parameters, i.e. for given outer density and temperature. This fact leads to another description of the phenomenon, also used in this article (cf. Fig. 1), presenting a manifold of possible static core–envelope structures in a parameter set of core mass

*Tel.: +49 6221 3282970.
E-mail address: schoenke@ita.uni-heidelberg.de.

0032-0633/$ - see front matter © 2007 Elsevier Ltd. All rights reserved.
doi:10.1016/j.pss.2007.04.002

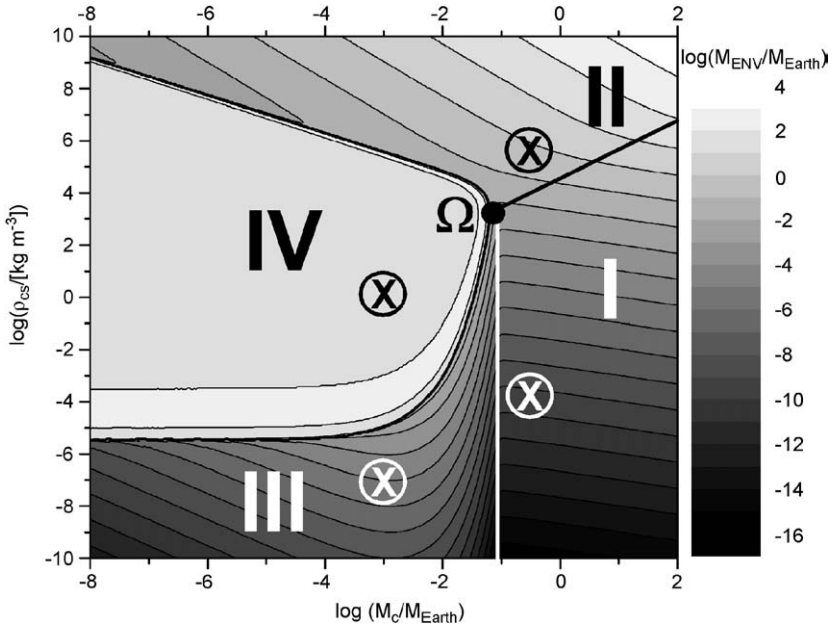

Fig. 1. Contour plot of envelope mass at the Hill radius, function of core mass M_c and gas density ρ_{cs} at core surface. Parameters are given in the text.

M_c and gas density (or pressure) at the core surface ρ_{cs} (Broeg, 2006; Pečnik and Wuchterl, 2005). In this description we find the point of CCM if we fix the outer temperature and follow a line of constant outer density in the direction of increasing total mass. We will reach at least one maximum in the core mass, corresponding exactly to the classical CCM. A nice visualization how the $M_c(M_{tot})$-plot can be understood as a projection out of the manifold is shown in Broeg (2006). It shows that the CCM is closely related to the highest core mass value of the so-called "region IV" in the described parameter set, our point Ω in Fig. 1. The direct connection to our work gives the isothermal investigation by Pečnik and Wuchterl (2005). Besides the local CCM, defined there as the outer density depending classical CCM, they introduce a global CCM which is independent of the outer density and corresponds again to our point Ω. In fact this global CCM is the classical CCM for the highest possible outer density permitting hydrostatic equilibrium. The finding that the classical CCM is quite independent of the outer density (Mizuno, 1980) can be explained with the strong decrease of the outer density for increasing core mass beyond the global CCM, the point Ω, because of the strong gravitational influence the core gets. So the global and classical CCMs do not differ significantly since all outer densities are realized in a short core mass range. But this behaviour changes for small orbital distances (Ikoma et al., 2001) or fully convective envelopes (Wuchterl, 1993). For small orbital distances this happens because the above-mentioned fast drop in outer density beyond the point Ω is slowed down due to increasing gas temperature. Naturally the global CCM has the smallest value under all possible CCMs with their respective nebula densities, since it is related to the highest outer density.

Being a main assumption of this article, the isothermal approximation has to be discussed. As all attempts to justify this assumption involve a lot of vague estimations about opacity, luminosity and other temperature gradient related parameter values (e.g. Pečnik and Wuchterl, 2005), we choose a rather pragmatic way to show the applicability of the isothermal assumption. Clearly, for high densities especially in the compact near core parts of the envelope, significant temperature gradients appear. But in the parameter range of interest for this work, i.e. for densities up to $\rho \approx 1 \cdot 10^3\,\mathrm{kg\,m^{-3}}$ (cf. the "height" of the point Ω in Fig. 1), we justify the approximation by comparing our results with respective non-isothermal investigations. Critical density (cf. Section 4.1) as well as the global CCM (cf. Section 4.6) agrees up to a factor of 2 with the respective non-isothermal results. So the isothermal investigation provides more than just qualitative answers.

For a review of the whole topic cf. Wuchterl et al. (2000), for a detailed discussion of the critical mass cf. Wuchterl (1991).

1. The model and its equations

Our model contains a solid, rigid core, with mass M_c and mean density ϱ_c, so that we get the core radius

$$r_c = \sqrt[3]{\frac{3M_c}{4\pi\varrho_c}}.$$

The envelope starts at r_c with a given density $\rho(r_c) \coloneqq \rho_{cs}$ (gas density at the core surface). To describe the mass distribution $M(r)$ and density profile $\rho(r)$ in the envelope, we need the following equations. The force density balance

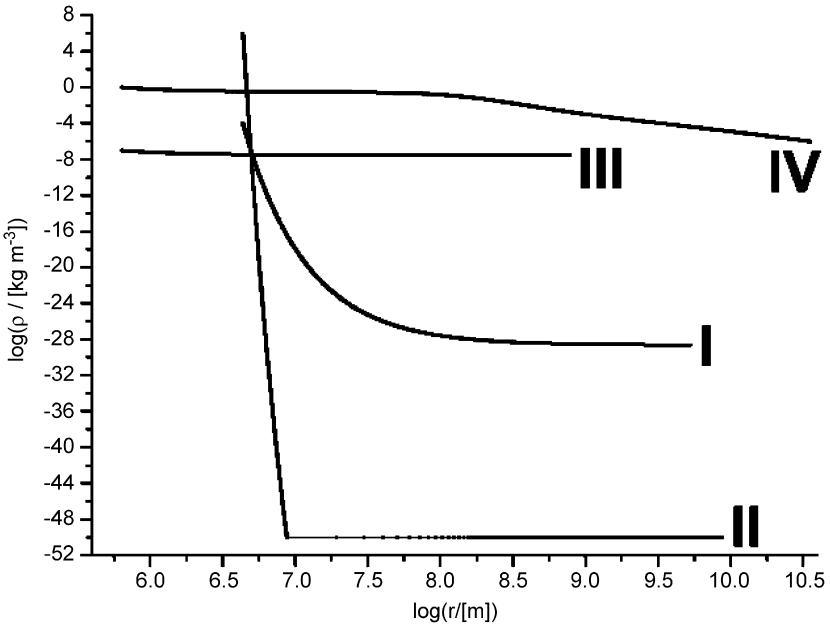

Fig. 2. Examples for radial density profiles for the four different regions in Fig. 1.

for the hydrostatic equilibrium is

$$\nabla P = -\rho \nabla \phi,$$

where P is the gas pressure and ϕ the gravitational potential. In radial symmetry and with

$$\nabla \phi = -\mathbf{f}_g = \frac{GM}{r^2}\frac{\mathbf{r}}{r},$$

with $\mathbf{f}_g$ the specific gravitational force, we get

$$\frac{dP(r)}{dr} = -\frac{GM(r)\rho(r)}{r^2}. \quad (1)$$

In addition, we need the equation of state for the ideal gas in the isothermal case[1]

$$P(r) = \frac{k_B T}{m_g}\rho(r), \quad T = \text{const}, \quad (2)$$

with m_g the atomic mass of one gas particle. Introducing (2) in (1) we obtain

$$\frac{d\rho(r)}{dr} = -\frac{Gm_g}{k_B T}\frac{M(r)\rho(r)}{r^2}. \quad (3)$$

Mass density $\rho(r)$ and mass distribution $M(r)$ are related by

$$\frac{dM(r)}{dr} = 4\pi r^2 \rho(r). \quad (4)$$

Together, Eqs. (3) and (4) represent a nonlinear system of ordinary differential equations, whose solutions are uniquely determined given the two initial conditions $M(r_c) = M_c$ and $\rho(r_c) = \rho_{cs}$.

[1]Up to $\rho \approx 1 \cdot 10^3\,\mathrm{kg\,m^{-3}}$, the assumption of ideal and isothermal gas is a valid approximation. For an extensive discussion of the applicability of ideal gas and the isothermal assumption cf. Pečnik and Wuchterl (2005).

2. The numerical results so far and the questions they raise

The system (3), (4) has previously been examined with numerical methods, cf. Pečnik and Wuchterl (2005), Schönke (2005). The integration was always stopped at the so-called Hill radius $r_H = a\sqrt[3]{M(r_H)/3M_S}$, where a is the planet's orbital distance from the central star, $M(r_H)$ the mass at the Hill radius (i.e. the total mass M_{tot}) and M_S the mass of the star. r_H approximates the region of gravitational influence of the planet (cf. Section 4.4). Fig. 1 shows the envelope mass at the Hill radius $M_{env} = M_{tot} - M_c$, for a variety of values of M_c and ρ_{cs} ($a = 5.2\,\mathrm{AU}$, $T = 123\,\mathrm{K}$, $M_S = \mathrm{M}_\odot$, $\varrho_c = 5500\,\mathrm{kg\,m^{-3}}$, $m_g = 3.32 \cdot 10^{-27}\,\mathrm{kg}$ (molecular hydrogen)).

We can distinguish four different regions. The crosses in Fig. 1 mark the M_c and ρ_{cs} values, for which we see a radial density profile in Fig. 2, one for each region. The density $\rho(r_H)$ at distance $r = r_H$ from the planet connects to the nebula density, so if we embed the planet in a certain nebula, we have to choose the right profile. Now, we give a very short summary of the nature of the different regions. Region I ("earth-like planets") has massive cores compared to the mass of the envelope, the gravitational potential is dominated by the core and the density decreases exponentially with radius (like on earth with our atmosphere as the envelope). Region II ("gas giant planets") has high ρ_{cs} values, so there is so much mass in the envelope near the core, that self-gravity of the gas sets in and forms a compact envelope; for radii further out, the density drops very fast to vacuum. Profile II in Fig. 2 is set constant to $\log\rho = -50$ (perfect vacuum) where integration gives smaller values. Region III ("asteroids") has small cores, which hardly influence the surrounding gas so that the envelope is quasi-homogenous, i.e. $\rho(r_c) \approx \rho(r_H)$. Region IV ("protoplanets") has massive and extended envelopes,

which get self-gravitating beyond some radial distance (the density decrease changes from exponential to $1/r^2$, cf. the bend in the profile IV of Fig. 2), but are not compact yet. At a specific ρ_{cs} value, the near core parts of the envelope become compact in a local sense, but do not influence the whole structure.

The question is how to make a clear statement about where the transition occurs between, e.g. region III and I. Precisely, if we assume the border between III and I in Fig. 1 to be vertical: which minimal mass does a core need, so we can call it an "earth-like planet" rather than an "asteroid"? Another question concerns the problem where we can find the so-called point of critical mass (Ω in Fig. 1), defined to be the point where the four regions in Fig. 1 meet? This point should lie on the upper end of the border line between III and I, of course, and its ρ_{cs} should be equal to the specific value, for which objects in IV get locally compact near the core. But which value is it? The procedure so far was to plot something like Fig. 1 and to tell the points from this graphic. But this is unsatisfactory, because we do not know what happens, if we change the temperature or other important variables, like the orbital distance (which will also change the temperature), the density of the core or the atomic weight of the gas. What happens at these border lines and at Ω in particular? Why such a sudden change in the qualitative behaviour? To answer these questions we need a new representation of the system (3), (4) and an analytical expression for Ω, depending on quantities like the above-mentioned ones. In the following, we delineate a way to achieve these goals.

3. Mathematical preparations

This section is a rather technical part. It discusses the transformation of the original system into an autonomous one, i.e. a system which does not contain the independent variable explicitly. In this form, we can represent all solutions in terms of a phase portrait which gives us a deeper insight into the system's properties. The application to the physical problem starts with Section 3.3. The reader not interested in the mathematical reasoning may skip the other sections.

3.1. Transformation to a generalized Emden–Fowler equation

First, we introduce dimensionless variables

$$r = r_0 x, \quad M(r) = M_\oplus z(x), \quad \rho(r) = \varrho_c y(x),$$

where $M_\oplus = 5.976 \cdot 10^{24}\,\mathrm{kg}$ is the earth mass, ϱ_c is the mean density of the core and $r_0 = \sqrt[3]{3M_\oplus/(4\pi\varrho_c)}$. So now, (3) and (4) become

$$\frac{\mathrm{d}y}{\mathrm{d}x} = -C\frac{yz}{x^2}, \tag{5}$$

$$\frac{\mathrm{d}z}{\mathrm{d}x} = 3x^2 y, \tag{6}$$

$C = 6^{2/3}\pi\,1/3GM_\oplus^{2/3}\varrho_c^{1/3}m_g/3k_BT \approx 4.259 \cdot 10^2((\varrho_c/[\mathrm{kg\,m^{-3}}])^{1/3}\ (m_g/[\mathrm{u}])/(T/[\mathrm{K}]))$, $(u = 1.66 \cdot 10^{-27}\,\mathrm{kg}$ (atomic mass unit)). The transformation of the independent variable x into a kind of "volume-like" variable v in the form

$$v = x^3 \Rightarrow \mathrm{d}v = 3x^2\,\mathrm{d}x = 3v^{2/3}\,\mathrm{d}x, \tag{7}$$

changes (5) and (6) into

$$\frac{\mathrm{d}y}{\mathrm{d}v} = -\frac{C}{3}\frac{yz}{v^{4/3}}, \tag{8}$$

$$\frac{\mathrm{d}z}{\mathrm{d}v} = y. \tag{9}$$

If we differentiate (9), $z'' = y'$, we can introduce this into (8) and change the system of two first-order differential equations into one second-order equation

$$\frac{\mathrm{d}^2 z}{\mathrm{d}v^2} = -\frac{C}{3}v^{-4/3}z\frac{\mathrm{d}z}{\mathrm{d}v}. \tag{10}$$

This is a generalized Emden–Fowler equation, i.e. a special case of $\ddot{s} = At^n s^m \dot{s}^l$ with $A, n, m, l \in \mathbb{R}$. In our case $n = -4/3$, $m = 1$, $l = 1$ (and $A = -C/3$),[2] no analytical solution is known so far. (For other combinations of n, m, l, there exists information about solutions, mainly in parametric form. In addition, a general procedure for arbitrary n, m, l is known, which reduces this kind of equations to an Abel equation of the second kind, but this again is not analytically solvable cf. Polyanin and Zaitsev (2003).) However, a particular solution can always be given which has no free constants of integration and describes the asymptotic behaviour of the general solution. This solution will play an important role in the following. More details about generalized Emden–Fowler equations are given in Polyanin and Zaitsev (2003).

3.2. Reduction to an autonomous dynamical system via point transformations

To extract the asymptotic behaviour of z at large values of v, we make the ansatz[3]

$$\tilde{z} = v^{-\alpha}z, \quad \tilde{v} = \ln v, \tag{11}$$

where α is a free parameter. Using (11) together with

$$\frac{\mathrm{d}z}{\mathrm{d}v} = v^{\alpha-1}\left(\alpha\tilde{z} + \frac{\mathrm{d}\tilde{z}}{\mathrm{d}\tilde{v}}\right), \tag{12}$$

$$\frac{\mathrm{d}^2 z}{\mathrm{d}v^2} = v^{\alpha-2}\left[\alpha(\alpha-1)\tilde{z} + (2\alpha-1)\frac{\mathrm{d}\tilde{z}}{\mathrm{d}\tilde{v}} + \frac{\mathrm{d}^2\tilde{z}}{\mathrm{d}\tilde{v}^2}\right], \tag{13}$$

in (10), we obtain

$$v^{\alpha-2}[\cdots] = -\frac{C}{3}v^{2\alpha-7/3}\left(\alpha\tilde{z} + \frac{\mathrm{d}\tilde{z}}{\mathrm{d}\tilde{v}}\right)\tilde{z}. \tag{14}$$

[2]The factor A is unimportant, it can always be changed to unity with the transformation $s \to A^{1/(1-m-l)}\tilde{s}$ (if $m + l \neq 1$).

[3]That (11) extracts the asymptotic behaviour is not obvious, it will turn out later that it is just the case.

As α is a free parameter, we can choose it in such a way that the exponents of v in (14) are equal on both sides of the equation, i.e. demanding

$$\alpha - 2 = 2\alpha - \tfrac{7}{3} \Rightarrow \alpha = \tfrac{1}{3}.$$

With (14), we have our requested autonomous equation

$$\frac{\mathrm{d}^2\tilde{z}}{\mathrm{d}\tilde{v}^2} = \frac{1}{3}\frac{\mathrm{d}\tilde{z}}{\mathrm{d}\tilde{v}} - \frac{C}{3}\frac{\mathrm{d}\tilde{z}}{\mathrm{d}\tilde{v}}\tilde{z} + \frac{2}{9}\tilde{z} - \frac{C}{9}\tilde{z}^2. \tag{15}$$

From Eq. (15), it is straightforward to construct the autonomous dynamical system. But some care must be taken in the choice of our second variable $\tilde{y}$, which is needed to form a first-order system again. The simplest choice, $\tilde{y} = \mathrm{d}\tilde{z}/\mathrm{d}\tilde{v}$, would lead us to negative $\tilde{y}$ for some y range, as can be seen with (9) and (12). A much better alternative, showing analogies to the z transformation (11) (as we will see later), is

$$\frac{\mathrm{d}\tilde{z}}{\mathrm{d}\tilde{v}} = \tilde{y} - \frac{1}{3}\tilde{z}, \tag{16}$$

$$\Rightarrow \quad \frac{\mathrm{d}^2\tilde{z}}{\mathrm{d}\tilde{v}^2} = \frac{\mathrm{d}\tilde{y}}{\mathrm{d}\tilde{v}} - \frac{1}{3}\frac{\mathrm{d}\tilde{z}}{\mathrm{d}\tilde{v}} = \frac{\mathrm{d}\tilde{y}}{\mathrm{d}\tilde{v}} - \frac{1}{3}\tilde{y} + \frac{1}{9}\tilde{z}, \tag{17}$$

which keeps $\tilde{y}$ always positive (use (9) and (12) to prove that). Introducing (16) and (17) into (15), we get

$$\frac{\mathrm{d}\tilde{y}}{\mathrm{d}\tilde{v}} = \frac{1}{3}\tilde{y}(2 - C\tilde{z}). \tag{18}$$

Eqs. (16) and (18) represent our dynamical system.

3.3. A physical approach to the problem

With the information accumulated in the last sections, we have the opportunity to review the problem in a clear way. We define the dimensionless quantity

$$\varphi(r) \coloneqq \frac{Gm_\mathrm{g}}{k_\mathrm{B}T}\frac{M(r)}{r}, \tag{19}$$

which is obviously a *global gravitational potential*[4] divided by the thermal energy, and

$$\psi(r) \coloneqq \frac{Gm_\mathrm{g}}{k_\mathrm{B}T} 4\pi r^2 \rho(r), \tag{20}$$

which is a bit more complicated to describe. With (4), we see that $\psi \propto \mathrm{d}M/\mathrm{d}r$, which is the differential mass increase. But ψ is also something else, namely a *local gravitational potential* (again divided by the thermal energy). It is a measure for the gravitational interaction of neighbouring mass shells and therefore an indicator for self-gravity. We will see that the whole structure of the envelope can be understood by investigating the interplay of the two potentials φ and ψ. Introducing (19) and (20) into (3) and (4) and then substituting the independent variable

$$s \coloneqq \ln(r/r_\mathrm{c}), \tag{21}$$

we obtain

$$\frac{\mathrm{d}\varphi}{\mathrm{d}s} = \psi - \varphi, \tag{22}$$

$$\frac{\mathrm{d}\psi}{\mathrm{d}s} = \psi(2 - \varphi). \tag{23}$$

The system (22), (23) has the same structure as (16), (18), i.e. it is an autonomous dynamical system. The advantage now is that we have a clear picture of the quantities φ and ψ, in contrast to $\tilde{z}$ and $\tilde{y}$ in the last sections (but as a matter of fact, $\tilde{z}$ and φ or rather $\tilde{y}$ and ψ are identical up to a factor).

3.4. Connections to homology invariants

A comparison of our variables with the well-known homology invariants U and V, given by (e.g. Kippenhahn and Weigert, 1990)

$$U \coloneqq \frac{\mathrm{d}\ln M}{\mathrm{d}\ln r} = \frac{4\pi r^3\rho}{M}, \tag{24}$$

$$V \coloneqq -\frac{\mathrm{d}\ln P}{\mathrm{d}\ln r} = \frac{\rho}{P}\frac{GM}{r}, \tag{25}$$

shows some similarity. Since we consider an ideal gas, i.e. $\rho/P = m_\mathrm{g}/(k_\mathrm{B}T) = \mathrm{const}$ (cf. (2)), a comparison of (24) and (25) with (19) and (20) leads to

$$\varphi = V, \quad \psi = UV. \tag{26}$$

So φ and ψ are homology invariants as well, because the product UV is still an invariant quantity. In fact all homology invariants lead (together with (21)) to autonomous systems of differential equations. Maintaining homology, i.e. to ensure a kind of similarity between different solutions of a system, requires the spatial independence of the evolution of the invariants.

With the variables U and V we obtain a much more complicated system than (22) and (23). Our equations contain only one non-linearity (the term $-\psi\varphi$ in (23)), whereas in the $U - V$ variables we would get quadratic terms. No combination of the invariants was found leading to "simpler" expressions than (22) and (23).

4. Properties of the system

There are two important critical lines in the system (22), (23) (the third critical line, $\psi = 0$ is trivial: $\rho = 0$), namely

$$\psi = \varphi \quad [\text{with } \mathrm{d}\varphi/\mathrm{d}s = 0], \tag{27}$$

$$\varphi = 2 \quad [\text{with } \mathrm{d}\psi/\mathrm{d}s = 0], \tag{28}$$

describing extrema of φ and ψ, respectively. These lines together with the phase portrait of the system are shown in Fig. 3. All information about the radial profiles $M(r)$ as well as $\rho(r)$ is contained in the figure. Given initial conditions M_c, ρ_cs and r_c (via ϱ_c), we obtain from (19) and (20) an initial point $(\varphi_\mathrm{c}, \psi_\mathrm{c})$ in Fig. 3.

[4] It is convenient to have φ as well as ψ positive by definition.

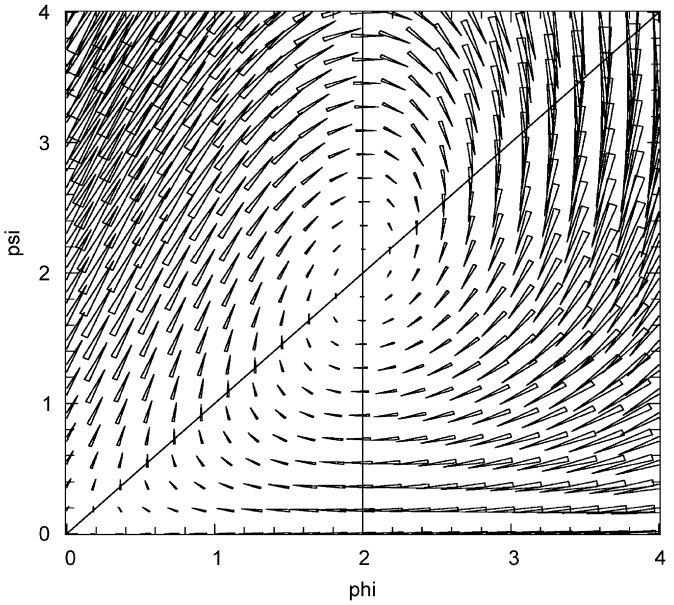

Fig. 3. Phase portrait for the system (22), (23), with the critical lines $\psi = \varphi$ and $\varphi = 2$.

As we are interested in positive values of φ and ψ, the most noticeable object in Fig. 3 is the global attractor at the point $(\varphi, \psi) = (2, 2)$, which follows from $\mathrm{d}\varphi/\mathrm{d}s = \mathrm{d}\psi/\mathrm{d}s = 0$ at this point, i.e. the two critical lines $\psi = \varphi$ and $\varphi = 2$ intersect there, and the fact that every initial point $(\varphi, \psi) \in \mathbb{R}^+ \times \mathbb{R}^+$ is drawn to it for $s \to \infty$ (ignoring that we stop at the Hill radius $s_\mathrm{H} \propto \ln r_\mathrm{H}$). With (19) and (20) we see immediately that $(\varphi, \psi) = (2, 2) = \text{const}$ is related to the profiles $\rho \propto 1/r^2$ and $M \propto r$, which were said to be typical for the self-gravitating, noncompact parts of profiles in region IV (cf. Section 2). That means that all profiles in all regions would have such a part, if their Hill radius were not reached or they had not become compact before. In general, every gas sphere, with or without a core, would evolve into this asymptotic structure, for big radii.[5] In these envelope parts the gas interacts with its local vicinity only. The solution at (2, 2) is the particular solution, mentioned in Section 3.1. Our transformations (19), (20) extracted the asymptotic behaviour $\rho \propto 1/r^2$ and $M \propto r$ from the original variables ρ and M.

4.1. The critical density

The first critical line (27) describes the points where an important event takes place: the strength of ψ becomes equal to the strength of φ. Introducing (19) and (20) into (27), we get a critical density

$$\rho_\mathrm{crit}(r) = \frac{M(r)}{4\pi r^3} = \frac{\langle \rho(r) \rangle}{3}, \tag{29}$$

where $\langle \rho(r) \rangle$ denotes the mean density inside the sphere of radius r. Whenever the local density reaches one third of the mean density, local self-gravity has the same influence on the gas as the total mass inside the actual sphere. For $\psi > \varphi$, the local self-gravity of the gas dominates the global gravitational potential. Here, we see a fundamental conclusion for all isothermal core–envelope configurations in radial symmetry. Applied to the core surface, with $\langle \rho(r_\mathrm{c}) \rangle = \varrho_\mathrm{c}$, the critical density ρ_crit is nothing else but the specific ρ_cs value in region IV, mentioned in Section 2, because with the local self-gravity beginning to overrule the global potential at the core surface, we just have the property which distinguishes between a core-gravity resp. a self-gravity dominated core surface, which was said to be the basic difference between planets below resp. above the point $\boldsymbol{\Omega}$ in Fig. 1, Section 2. Therefore ρ_crit is one coordinate ρ_Ω of the point $\boldsymbol{\Omega}$!

$$\rho_\Omega = \frac{\varrho_\mathrm{c}}{3}. \tag{30}$$

The beauty of this important result arises from its incredible simplicity! There is a specific density, for which the gas at core surface starts to show self-gravity effects. This critical density is reached, when it is exactly one third of the mean density of the rigid core (which can have arbitrary density distribution). For this transition point, we find yet another change in the stability behaviour, as a new instability sets in and amplifies the already existing instability (cf. Schönke, 2005). The comparison of (30) with isothermal numerical results shows exact agreement (e.g. Pečnik and Wuchterl, 2005). Non-isothermal investigations by Broeg (2006), including detailed EOS and energy transfer, contain characteristic values for gas pressure and temperature at the core surface for the corresponding point Ω. Using the respective EOS, we get the critical density at the core surface for that point. Interestingly, this critical density has the same value for different states, i.e. different temperatures and pressures at the core surface (due to, e.g. different nebula parameters). This is a clear agreement with our result that the critical density exclusively depends on the core density. The non-isothermal value is approximately $1000\,\mathrm{kg\,m^{-3}}$, whereas we get $\frac{5500}{3}\,\mathrm{kg\,m^{-3}} \approx 1800\,\mathrm{kg\,m^{-3}}$. The reason for the generally smaller non-isothermal value seems to be a non-trivial question which cannot be answered so far.

4.2. The minimum core mass

If we define a specific, asymptotic energy

$$\varepsilon := \frac{2k_\mathrm{B}T}{m_\mathrm{g}}, \tag{31}$$

the second critical line (28) can be identified with (using (19))

$$\frac{GM(r)}{r} = \varepsilon. \tag{32}$$

The term "asymptotic energy" should become clear after looking at the asymptotic solutions of the trajectories of our system: As we get closer to the attractor, GM/r tends towards

[5] Because of the outer boundary (Hill radius), only profiles in region IV have this structure.

ε (i.e. $\varphi \to 2$). If $GM/r > \varepsilon$ ($\varphi > 2$), a gas particle feels a stronger force $\mathbf{F}_g = -GMm_g\mathbf{r}/r^3$ towards the centre than in the asymptotic case, whereas the force is lower if $GM/r < \varepsilon$ ($\varphi < 2$).

Again applied to the core surface ($M = M_c$, $r = r_c$), the condition (32) leads us to a *minimum core mass*

$$M_c^{\min} = \left(\frac{3}{4\pi\varrho_c}\right)^{1/2}\left(\frac{\varepsilon}{G}\right)^{3/2} = \left(\frac{3}{4\pi\varrho_c}\right)^{1/2}\left(\frac{2k_BT}{Gm_g}\right)^{3/2}. \quad (33)$$

At a core mass of $M_c^{\min}$ the envelope at the core surface "feels" like it is far away from the core and evolves in the asymptotic way. Core masses smaller than $M_c^{\min}$ have practically no influence on the envelope, the gas reacts on the "lacking potential" even with a small density excess at the core surface. In general, *with a value of* $M_c^{\min}$, *a core starts to influence the envelope*, *it is the* "core mass" *analogue to* ρ_Ω. The counterpart of this border line, representing $M_c^{\min}$, is not so obvious in Fig. 1 because the plot shows the envelope mass at the Hill radius, and the inner envelope structure is hidden in this global property. Nevertheless $M_c^{\min}$ can be found in form of the line connecting the minima of the contour lines in region III at $\log(M_c^{\min}/M_\oplus) = -2.85$. These minima correspond to maxima in the envelope mass M_{env}. For $M_c < M_c^{\min}$, M_{env} increases with M_c due to the growing Hill radius caused by the increasing (but not yet important) core mass. For $M_c > M_c^{\min}$, the core forces the density to decrease faster near the core to maintain hydrostatic equilibrium, and M_{env} decreases.

4.3. Oscillations in the asymptotics

The outer envelope parts of the objects in region IV are a good example for the interplay between the potentials φ and ψ. An interesting feature of these envelopes, related to the asymptotic solutions and not mentioned in Section 2, is a damped oscillation first observed by Pečnik (2001). The density profiles $\rho(r)$, e.g. are oscillating around $1/r^2$ and reach it for $r \to \infty$ (this can hardly be suspected from Fig. 2, the picture is too small). An example for such a density profile in region IV is shown in Fig. 4. To discuss this feature, we investigate the vicinity of the attractor, i.e. perform a linearization of the phase portrait at the critical point. The two eigenvalues of the linearized system are

$$\lambda_{1,2} = \tfrac{1}{2}(-1 \pm i\sqrt{7}), \quad (34)$$

which show us, that φ and ψ behave like a damped oscillator, i.e. $\propto \exp[(-1/2 \pm i\sqrt{7}/2)s]$. It means that there is an alternating up and down of global and local gravitational energy, as a profile evolves outwards. This is obviously a critical situation for the envelope: it periodically starts some kind of self-interaction (i.e. self-gravity), but it is always a *local* phenomenon, instead of a compact state (which would be global). This behaviour is a hint that these kinds of envelopes may not be stable objects, which has indeed been found (cf. Schönke, 2005).

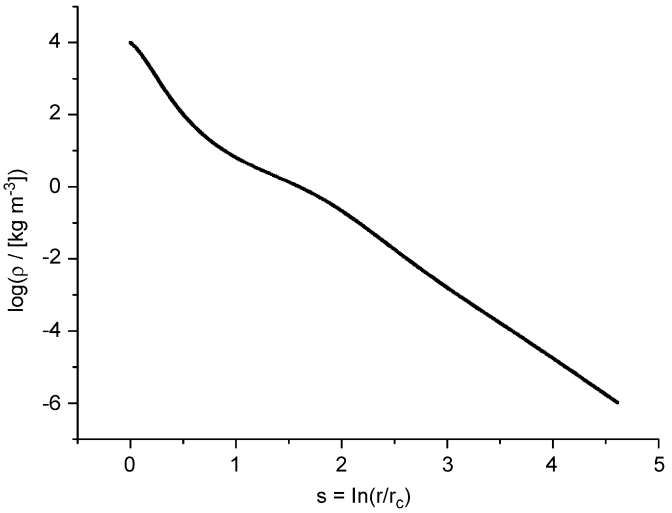

Fig. 4. Example for the damped oscillation of density profiles in region IV. The core mass is 10^{22} kg.

Out of curiosity, we calculate the wavelength of the oscillation. From (34), we tell the (dimensionless) wavenumber $k = \sqrt{7}/2$ and therefore the wavelength $\Lambda_s = 2\pi/k = 4\pi/\sqrt{7} \approx 4.75$, so we get the "real" wavelength $\Lambda_r = e^{\Lambda_s} = e^{4\pi/\sqrt{7}} \approx 115$, which is not a length[6] but tells us, if we started at an arbitrary radius r_0, that we went through one period after reaching $115\,r_0$.

4.4. The Hill radius

Most of the structures in Fig. 1, like the shapes of the different regions and their borders, discussed in Section 2, are strongly related to the choice of the outer boundary of the envelope. Especially the border lines between region III and IV as well as I and III, and therefore the CCM M_Ω, depend on this choice, in contrast to ρ_{crit} or $M_c^{\min}$, which are not influenced by the outer boundary, but represent points of fundamental changes concerning the inner structure of a core–envelope configuration. We use the Hill radius

$$r_H(M(r)) = a\sqrt[3]{M(r)/3M_S}, \quad (35)$$

as the outer boundary of the envelope. r_H describes the region of gravitational influence of the planet. In fact, it presents the oscillating sphere of the surface where the gradient of the effective potential[7] vanishes. The key problem of the incorporation of r_H is its dependence on $M(r)$ (cf. (35)) which in turn depends on r_H.

4.5. The border line between III and IV

The way to understand the border line structure of region IV is to ask the following question: Suppose we are

[6]Due to the autonomous equations we "lost" the length scale, the system is invariant under scaling of r.

[7]$\phi_{eff} = \phi_{star} + \phi_{planet} + \phi_{centrifugal}$ in the corotating system.

exactly at the Hill radius. If we make another radial step dr outwards, do we get so much more mass dM, that the new Hill radius $r_H(M+dM)$ equals our new position $r_H(M)+dr$? This borderline case defines the boundary between region III and IV. The answer to the above question is either "No, we get even more mass, so the new r_H is bigger than our new position", if we are in region IV, or "No, we do not get enough new mass, so the new r_H is smaller than our new position", if we are in region III. It is clear that this explains the sudden increase in M_{env} at the boundary between the two regions: In region IV we can go further out, because r_H+dr is still inside the new Hill sphere, whereas in region III we have to stop, because otherwise we would leave the region of gravitational influence of the planet.

So we have to compare the differential mass increases at the Hill radius. With (35), the critical increase is

$$\frac{dM}{dr_H}=\frac{9M_S}{a^3}r_H^2. \tag{36}$$

The general mass increase at r_H is (using (4))

$$\left.\frac{dM}{dr}\right|_{r_H}=4\pi r_H^2\rho(r_H). \tag{37}$$

To find an expression for the outer gas density $\rho_H:=\rho(r_H)$, we can take advantage of the fact that there exists an analytic solution for the regions I and III, which is a perfect approximation, as long as we stay out of region II or IV. As a matter of fact, we use an approximation to find out where the approximation itself breaks down! As in region I and III the core mass is always at least a hundred times larger than the envelope's mass, we can say that the mass is constant and equal to the core mass. This procedure, known as the Roche approximation, simplifies (3) to

$$\frac{d\rho(r)}{dr}=-\frac{Gm_g}{k_BT}\frac{M_c\rho(r)}{r^2}, \tag{38}$$

which can be integrated easily

$$\rho(r)=\rho_{cs}\exp\left[\frac{Gm_gM_c}{k_BT}\left(\frac{1}{r}-\frac{1}{r_c}\right)\right],$$

$$\rho_H:=\rho(r_H)=\rho_{cs}\exp\left[\frac{Gm_gM_c}{k_BT}\left(\frac{1}{r_H}-\frac{1}{r_c}\right)\right].$$

After eliminating r_c and r_H we get[8]

$$\rho_H=\rho_{cs}\exp\left(\frac{Gm_g}{k_BT}\left[\frac{(3M_S)^{1/3}}{a}-\left(\frac{4\pi\varrho_c}{3}\right)^{1/3}\right]M_c^{2/3}\right). \tag{39}$$

If we introduce (39) into (37) and then equate (36) and (37), we find

$$\frac{9M_S}{a^3}=4\pi\rho_{cs}\exp\left(\frac{Gm_g}{k_BT}\left[\frac{(3M_S)^{1/3}}{a}-\left(\frac{4\pi\varrho_c}{3}\right)^{1/3}\right]M_c^{2/3}\right),$$

and the border line between region III and IV to be

$$\rho_{cs}^{III,IV}(M_c)=\frac{9M_S}{4\pi a^3}\exp\left(\frac{Gm_g}{k_BT}\left[\left(\frac{4\pi\varrho_c}{3}\right)^{1/3}-\frac{(3M_S)^{1/3}}{a}\right]M_c^{2/3}\right). \tag{40}$$

For $M_c\to 0$ we get the critical central density of a gas sphere, above which it can build up an extensive envelope

$$\bar\rho:=\rho_{cs}^{III,IV}(M_c\to 0)=\frac{9M_S}{4\pi a^3}, \tag{41}$$

which is called $\bar\rho$, because it is the mean density $\langle\rho(r_H)\rangle$ of an object, cf. (29) and (35) (all models have the same $\bar\rho$ for fixed a and M_S). It is also the highest possible outer density of any envelope. Actually, the outer density equals $\bar\rho$ for every point on the border line of region IV (towards region III and region II) in the approximation (38). There are no static solutions for outer densities higher than $\bar\rho$, therefore $\bar\rho$ is a critical nebula density, a density analogue to the CCM.

4.6. The critical core mass

With the knowledge of the critical density at the core surface ρ_Ω (cf. Section 4.1), it is now straightforward to calculate the CCM M_Ω with the help of (40). We just need to ask for the M_c value where the borderline between III and IV crosses the critical density ρ_Ω, i.e. we have to solve the equation $\rho_{cs}^{III,IV}(M_\Omega)=\rho_\Omega=\varrho_c/3$, giving

$$M_\Omega=\left(\frac{\frac{k_BT}{Gm_g}\ln\left(\frac{4\pi a^3\varrho_c}{27M_S}\right)}{\left(\frac{4\pi\varrho_c}{3}\right)^{1/3}-\frac{(3M_S)^{1/3}}{a}}\right)^{3/2}. \tag{42}$$

With M_Ω we found the second and final coordinate of the point of critical mass Ω! We can think of M_Ω as the end of a process, which began with the minimum core mass. At M_c^{min} the core started to influence the envelope near the core, whereas at M_Ω the core interacts with the whole envelope up to the Hill radius. For the parameters like in Fig. 1, we get a CCM of $\log(M_\Omega/M_\oplus)\approx -1.17$, in excellent agreement to numerical results from other isothermal investigations (Pečnik and Wuchterl, 2005). The obvious discrepancy to non-isothermal publications (Mizuno, 1980; Ikoma et al., 2001), which give values up to the order of $10M_\oplus$, has three main reasons. As mentioned before, M_Ω is the global CCM, i.e. the CCM for the highest possible outer density $\bar\rho$ and therefore the minimum CCM value for all possible nebula densities (cf. Introduction). But if we look into Fig. 1 in Ikoma et al. (2001), we can actually find the respective M_Ω value. There, the classical CCM is shown at 0.1 AU for different nebula densities up to $1000\,\rho_0^H\approx 0.67\,kg\,m^{-3}$ (ρ_0^H is the MMSN density, Hayashi et al., 1985) which is close to but already above the (isothermal) maximum outer density of $\bar\rho=0.42\,kg\,m^{-3}$ at that orbital distance (cf. (41)). For $1000\,\rho_0^H$, i.e. the very right end of the graph, the CCM is given as

[8] If $a>0.1$ AU (with $M_S=M_\odot$, $\varrho_c=\varrho_\oplus$), then $r_H\gg r_c$ and the term $(3M_S)^{1/3}/a$ is negligible in all the forthcoming formulas.

$M_c^{crit} \approx 0.55 M_\oplus$, where (42) with the respective parameters gives $M_\Omega = 0.38 M_\oplus$, which is not such a big deviation anymore. The second reason for the still remaining difference is of course the isothermal assumption giving naturally smaller values for the CCM because the constant temperature is certainly a lower limit for the planet especially in the high density parts close to the core. Upcoming analytic investigations with polytropic relations (to be published soon) will show significantly increased values for M_Ω. Last but not least there are deviations due to non-ideal effects of the gas not considered in this article.

4.7. The border line between I and III

As we mentioned before, M_Ω also represents the border line between the regions I and III, i.e.

$$M_c^{I,III} = M_\Omega, \tag{43}$$

so an object with $M_c > M_\Omega$ can be called an "earth-like planet" and its core holds the envelope in a "firm grip". If we define a density contrast

$$\delta := \frac{\rho_{cs}}{\rho_H}, \tag{44}$$

we see with (39) that in region I and III, δ is constant for a constant core mass. At $M_c = M_\Omega$, we find

$$\delta_\Omega = \frac{4\pi a^3 \varrho_c}{27 M_S} = \frac{\rho_\Omega}{\bar\rho}. \tag{45}$$

Therefore, the ability to keep an atmosphere when the nebula is removed can also be described with a minimum density contrast of δ_Ω. If $\delta < \delta_\Omega$, we have just an "asteroid".

4.8. Properties of region IV

Profiles in region IV end up at $(\varphi, \psi) = (2, 2)$ sooner or later, as we mentioned before. The total mass and the outer density do not vary much in the whole region, as can be seen in Fig. 1. If we evaluate (19) and (20) for $(\varphi, \psi) = (2, 2)$ at $r = r_H$, we obtain the mean values for M_{env} (the height of the "island" in Fig. 1) and ρ_H in region IV

$$\langle M_{env}^{IV} \rangle = \left(\frac{2 k_B T a}{G m_g}\right)^{3/2} (3 M_S)^{-1/2}, \tag{46}$$

$$\langle \rho_H^{IV} \rangle = \frac{3 M_S}{4\pi a^3} = \frac{\bar\rho}{3}. \tag{47}$$

These values are exact at the point $(M_c, \rho_{cs}) = (M_c^{min}, \rho_\Omega)$, of course. The results are still correct for non-isothermal planets if only the outermost envelope parts are isothermal, as comparisons with Broeg (2006) show. The temperature to be inserted in (46) is then of course the one from the isothermal outer part, i.e. the nebula temperature. An interesting fact is that $\langle \rho_H^{IV} \rangle$ corresponds to the "mean density inside the orbit" (M_S distributed over a sphere with radius a), yet another property of the asymptotic solutions.

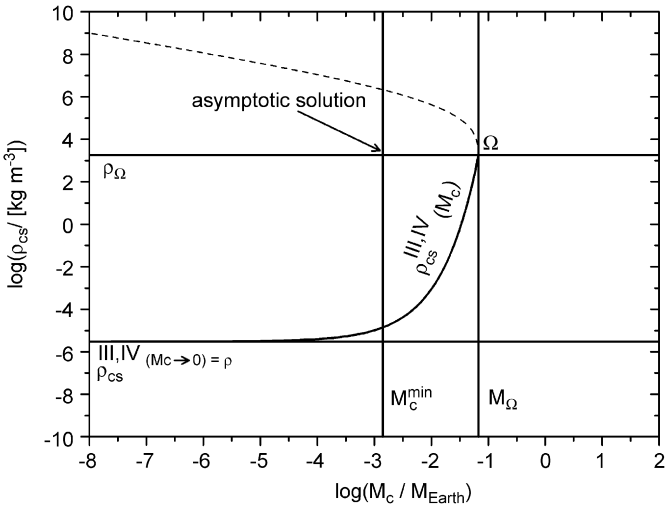

Fig. 5. Summary of the characteristic quantities, discussed in the previous sections, shown in the $M_c - \rho_{cs}$ parameter space (cf. Fig. 1).

4.9. A brief summary of the formulas

For an overall review, Fig. 5 collects the important quantities calculated so far. A comparison of its lines and points to the numerically computed structures in Fig. 1 shows excellent agreement. Using the abbreviations $C := (4\pi\varrho_c/3)^{1/3}$ and $D := (3M_S)^{1/3}/a = (4\pi\bar\rho/3)^{1/3}$ and $E := k_B T/(G m_g)$ we can summarize the derived formulas[9]

$$\rho_\Omega = \frac{\varrho_c}{3},$$

$$\bar\rho = \frac{9 M_S}{4\pi a^3},$$

$$M_c^{min} = \left(\frac{2E}{C}\right)^{3/2},$$

$$M_\Omega = \left[\frac{E}{C-D} \ln\left(\frac{\rho_\Omega}{\bar\rho}\right)\right]^{3/2},$$

$$\rho_{cs}^{III,IV}(M_c) = \bar\rho \exp\left(\frac{C-D}{E} M_c^{2/3}\right).$$

4.10. Dependence of the critical core mass on the orbital distance

It is interesting to investigate the dependence of M_Ω on the different parameters, especially the orbital distance a, because it usually changes the temperature, too. If we use a common temperature model for a solar nebula, e.g. by Hayashi et al. (1985)

$$\frac{T}{[K]} = 280 \left(\frac{L}{[L_\odot]}\right)^{1/4} \left(\frac{a}{[AU]}\right)^{-1/2}, \tag{48}$$

[9] If $a \gg (9M_S/4\pi\varrho_c)^{1/3}$, then $C \gg D$ and D can be neglected.

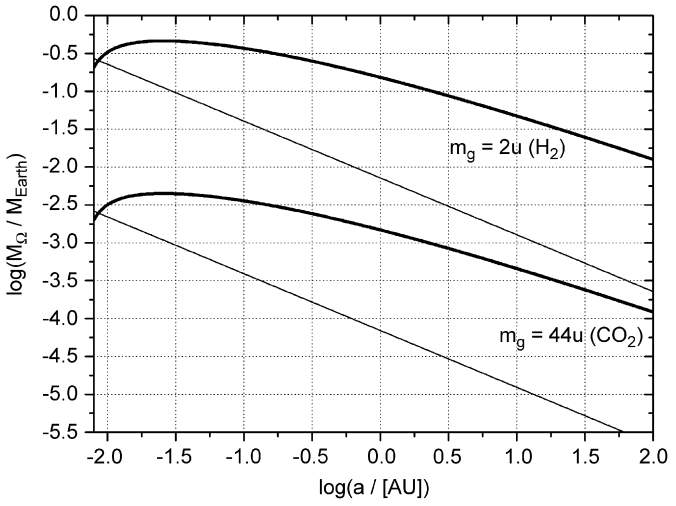

Fig. 6. The critical core mass M_Ω (thick lines) and the minimal core mass $M_c^{\min}$ (thin lines) as functions of orbital distance for two different molecular weights. The temperature dependence $T(a)$ is assumed to be (48). The molecular weight is just shifting the functions (cf. (42) and (33)).

with L as the luminosity of the central star, we can eliminate T and get a relation $M_\Omega(a) \propto a^{-3/4}[\ln(\kappa a)]^{3/2}$ with a constant κ depending on M_S and ϱ_c (cf. (42)). $M_\Omega(a)$ and $M_c^{\min}(a)$ are shown in Fig. 6 for two molecular weights (and $L = L_\odot$, other parameters like in Fig. 1). For $\log(a_0/[\mathrm{AU}]) \approx -2.07$, M_Ω equals $M_c^{\min}$. This happens because due to the decreasing orbital distance, $\bar{\rho}$ increases and gets close to ρ_Ω, the needed density contrast at the CCM becomes very small ($\delta_\Omega \approx 1$) and so does M_Ω. In contrast the minimum core mass increases continuously with decreasing orbital distance (or increasing temperature). For $a < a_0$ it is not possible to dominate an envelope with the core potential alone. Only compact objects (e.g. in region II with $\rho_{cs} > \rho_\Omega$) keep their envelopes when the nebula vanishes.

5. Conclusions

We investigated an isothermal core–envelope structure in radial symmetry as a model for a planet embedded in a nebula around a star. The underlying system of differential equations was transformed into an autonomous one, so we were able to represent a great variety of different solutions, i.e. radial profiles for mass and density, in a two-dimensional phase portrait with the trajectories as the solutions. This phase portrait is dissipative and contains a point attractor, so all trajectories tend towards the same limit. Thus all radial profiles exhibit an asymptotic "singular profile" for $r \to \infty$, which has the form $\rho \propto 1/r^2$ or rather $M \propto r$.

The transformed variables represent two kinds of gravitational potentials, one is the global potential φ and the other one is the local potential ψ describing self-gravity. The properties of the interplay between φ and ψ contain a lot of useful information.

An important result is the critical gas density above which self-gravity effects overrule the global gravitational potential. This happens when the local density is one third of the mean density inside the actual sphere. At the core surface this corresponds to one third of the mean core density and therefore gives us the density value ρ_Ω of the point of critical mass. If the gas density at the core is higher than ρ_Ω, self-gravity starts to influence the envelope in a global way. For the core mass we found the analogue to ρ_Ω in the minimal core mass $M_c^{\min}$. Cores more massive than $M_c^{\min}$ have a significant influence on the envelope.

Given a boundary for the region of gravitational influence in form of the Hill radius, we found the CCM M_Ω, marking the point where the core potential influences the whole Hill sphere. In the evolution of the protoplanetary disk, the value of M_Ω decides whether or not a planet is able to retain its gaseous envelope as the disk gas vanishes. Planets with cores above M_Ω will keep their envelope, while others will not (if not compact through self-gravity). The gas density analogue to M_Ω is the border line between region II and IV. As this line is not vertical, cf. Fig. 1, the critical gas density at the core surface, which ensures the transition to a compact state (i.e. entering region II), depends on the core mass. The bigger the core the smaller is the needed gas density (the core "supports" the compactification process).

The formulas derived for ρ_Ω and M_Ω describe the point of critical mass and therefore the important point where there are no more static states of the envelope in general and no more core growth driven, quasi-static evolution is possible.

The investigation of the behaviour of mass profiles $M(r)$ at the Hill radius led us to an explicit expression $\rho_{cs}(M_c)$ of the border line between "asteroids" in region III and "protoplanets" with extensive envelopes in region IV. For vanishing core mass, this relation gives the critical central density of a gas sphere, above which extensive envelopes are built up.

With the help of the asymptotic solutions we were able to determine the mean values of envelope mass and outer density for region IV. These quantities are quite constant there, because for $r \to r_H$ all profiles reach the unique asymptotic solution. Minor variations in the quantities at r_H are due to damped oscillations of the profiles near the asymptotic solution. These oscillations were investigated through linearization of the vicinity of the attractor in the phase portrait, including the calculation of the eigenvalues and the determination of the typical wavelength.

Acknowledgements

I want to thank Günther Wuchterl for the funny and interesting discussions and for showing me, what is really important when doing science; Bojan Pečnik for merging his thoughts with mine in times when something about our "island" seemed pretty strange; Dr. Herlt from the ITP of the physics department at the University of Jena, for a fruitful discussion about point transformations; Peter H. Richter, who encouraged me to write this treatise, although

I might do something different now and who gave me some useful hints for the discussion of the dynamical system; Werner M. Tscharnuter for some remarks, concerning connections to the homology invariants; the two unknown referees for helping to improve the clarity of the paper.

References

Broeg, C., 2006. Dissertation, Universität Jena.
Hayashi, C., Nakazawa, K., Nakagawa, Y., 1985. Protostars and Planets II, p. 1100.
Ikoma, M., Emori, H., Nakazawa, K., 2001. ApJ 553, 999.
Kippenhahn, R., Weigert, A., 1990. Stellar Structure and Evolution. Springer, Berlin.
Mizuno, H., 1980. Prog. Theor. Phys. 64, 544.
Papaloizou, J.C.B., Terquem, C., 1999. ApJ 521, 823.
Pečnik, B., 2001. Master Thesis, University of Zagreb.
Pečnik, B., Wuchterl, G., 2005. A&A 440, 1183.
Polyanin, A.D., Zaitsev, V.F., 2003. Exact solutions for ODE's, second ed. Chapman & Hall/CRC, London/Boca Raton.
Schönke, J., 2005. Diploma Thesis, Universität Jena.
Stevenson, D.J., 1982. PSS 30, 755.
Wuchterl, G., 1991. Icarus 91, 39.
Wuchterl, G., 1993. Icarus 106, 323.
Wuchterl, G., Guillot, T., Lissauer, J.J., 2000. Protostars and Planets IV, 1081.